# Rupture risk assessment for multiple intracranial aneurysms: why there is no need for dozens of clinical, morphological and hemodynamic parameters

Ther Adv Neurol Disord
2020, Vol. 13: 1–11
DOI: 10.1177/1756286420966159



**Belal Neyazi, Vanessa M. Swiatek, Martin Skalej, Oliver Beuing, Klaus-Peter Stein, Jörg Hattingen, Bernhard Preim, Philipp Berg, Sylvia Saalfeld§ and I. Erol Sandalcioglu§**

Correspondence to:
**Belal Neyazi**
Department of Neurosurgery, Otto-von-Guericke University, Leipziger Straße 44, Magdeburg, Saxony Anhalt 39120, Germany
**belal.neyazi@med.ovgu.de**

**Vanessa M. Swiatek**
Department of Neurosurgery, Otto-von-Guericke University, Magdeburg, Saxony Anhalt, Germany

**Martin Skalej**
**Oliver Beuing**
Department of Neuroradiology, Otto-von-Guericke University, Magdeburg, Saxony Anhalt, Germany

**Klaus-Peter Stein**
Department of Neurosurgery, Otto-von-Guericke University, Magdeburg, Saxony Anhalt, Germany

**Jörg Hattingen**
Institute of Neuroradiology, KRH Klinikum Nordstadt, Hanover, Niedersachsen, Germany

**Bernhard Preim**
Department of Simulation and Graphics, Otto-von-Guericke University, Magdeburg, Saxony Anhalt, Germany

**Philipp Berg**
Department of Fluid Dynamics and Technical Flows, Otto-von-Guericke University, Magdeburg, Saxony Anhalt, Germany;
Research Campus *STIMULATE*, Magdeburg, Germany

**Sylvia Saalfeld**
Department of Simulation and Graphics, Otto-von-Guericke University, Magdeburg, Saxony Anhalt, Germany;
Research Campus *STIMULATE*, Magdeburg, Germany

***Abstract***

**Introduction:** A multitude of approaches have been postulated for assessing the risk of intracranial aneurysm rupture. However, the amount of potential predictive factors is not applicable in clinical practice and they are rejected in favor of the more practical PHASES score. For the subgroup of multiple intracranial aneurysms (MIAs), the PHASES score might severely underestimate the rupture risk, as only the aneurysm with the largest diameter is considered for risk evaluation.

**Methods:** In this study, we investigated 38 patients harboring a total number of 87 MIAs with respect to their morphological and hemodynamical characteristics. For the determination of the best suited parameters regarding their predictive power for aneurysm rupture, we conducted three phases of statistical evaluation. The statistical analysis aimed to identify parameters that differ significantly between ruptured and unruptured aneurysms, show smallest possible correlations among each other and have a high impact on rupture risk prediction.

**Results:** Significant differences between ruptured and unruptured aneurysms were found in 16 out of 49 parameters. The lowest correlation were found for gamma, aspect ratio (AR1), aneurysm maximal relative residence time (Aneurysm_RRT_max) and aneurysm mean relative residence time. The data-driven parameter selection yielded a significant correlation of only two parameters (AR1 and the Aneurysm_RRT_max) with rupture state (area under curve = 0.75).

**Conclusion:** A high number of established morphological and hemodynamical parameters seem to have no or only low effect on prediction of aneurysm rupture in patients with MIAs. For best possible rupture risk assessment of patients with MIAs, only the morphological parameter AR1 and the hemodynamical parameter Aneurysm_RRT_max need to be included in the prediction model.

***Keywords:*** hemodynamics, morphology, multiple intracranial aneurysms, rupture risk assessment, unruptured intracranial aneurysms

Received: 12 July 2020; revised manuscript accepted: 21 September 2020.

## Introduction

Intracranial aneurysms (IAs) are vascular dilatations, which can lead to subarachnoid hemorrhage (SAH) with poor prognosis.[1–3] Furthermore, SAH is associated with significant socioeconomic consequences due to long-term disability and loss of productive life years.[4]

Multiple intracranial aneurysms [(MIAs) ⩾2 IAs] form an important subgroup occurring in about 20% of IA carriers.[5] MIAs are associated with cardiovascular risk factors like hypertension and smoking.[5–8] Several characteristics are described, which define this subgroup: MIAs appear more often in women and older patients;[5–8] patients

**I. Erol Sandalcioglu**
Department of Neurosurgery, Otto-von-Guericke University, Magdeburg, Saxony Anhalt, Germany
§The authors contributed equally to the study.

with MIAs are more likely to have a familial predisposition for IA formation and longitudinal studies showed a higher rate of aneurysm growth.[5,9,10] Furthermore, the discussion about the higher risk rupture of MIAs compared with singular IAs forms a controversy in the treatment decision of these patients.[11–15]

Over the last decade a huge number of morphological and hemodynamic parameters as predictive factors for aneurysm rupture has been introduced.[16–23] As a limitation, these studies do not specifically address the subgroup of MIAs. Furthermore, the amount of potential predictive factors is not practical and thus does not impact rupture risk assessment in clinical practice. As a consequence, treatment decisions in most neurovascular centers for MIAs are mainly based on the PHASES score. This is indeed practical but might severely underestimate the rupture risk for the MIA subgroup, as only the aneurysm with the largest diameter is considered for risk evaluation.[24] Another approach to estimate the rupture risk of IAs is the establishment of reliable regression models, which combine morphological and hemodynamic predictive factors. Namely, two regression models showed a high area under the curve (AUC) of 0.84 and 0.86, respectively.[20,25] Nonetheless, neither of these models addresses the different subgroups of IAs specifically.

We investigated how many parameters are necessary for aneurysm status prediction and how much prediction power the potential parameters have. We focused exclusively on morphological and hemodynamic parameters. Therefore, we raised the number of these parameters from 13 used by Xiang *et al.*[20] to 49 (21 morphological and 28 hemodynamic) parameters. Moreover, we aimed to keep the influence of patient characteristics on rupture of IAs as constant as possible by using data from 38 patients with MIAs, with one ruptured and at least one unruptured IA. Based on this unique approach, the patient characteristics do not influence the results, yet they allow a clear relation of both morphological and hemodynamic characteristics to rupture status. In our study, first, we investigated the statistical significance of the difference between ruptured intracranial aneurysms (RIAs) and unruptured intracranial aneurysms (UIAs) with respect to their parameters. We selected the most important (with respect to the predictive power) parameters for further analyses. In the second phase, we examined whether the parameters contain redundant information by calculating correlations between them. We chose the parameter combinations with low information overlap for a regression analysis, which should be able to predict the aneurysm rupture status.

## Materials and methods

After obtaining permission from the local ethics committee of the Hanover Medical School and the Otto-von-Guericke University, we retrospectively analyzed the data of all patients who presented with a SAH and were treated at our Neurovascular Center in Hanover and Magdeburg between 2012 and 2019. Inclusion criteria for this study were: all patients had at least two IAs, of which one had ruptured; all patients had undergone complete neuroradiological diagnostics including three-dimensional (3D) rotational angiography (RA) and the ruptured aneurysm was identified by intraoperative findings or computed tomography scan imaging. Patients who suffered from a SAH and did not present with another IA were excluded. In addition, all patients who had not undergone complete neuroradiological diagnostic were excluded. Furthermore, all patients who suffered from fusiform aneurysms, additional vascular anomalies (e.g. arteriovenous malformation, Moyamoya disease, dural arteriovenous fistula) or polycystic kidney disease were excluded.

A total of 38 patients harboring 87 IAs were included in this study; the mean age at SAH was 57.5 years. Patients characteristics are shown in Table 1.

### *Extraction of morphological and hemodynamic parameters*

From the reconstructed and digital subtracted 3D RA dataset, 3D surface models were extracted according to Saalfeld *et al.*[26] Next, we applied a semiautomatic neck curve segmentation, which also allows for the automatic extraction of 21 morphological parameters[27] (Figure 1, Table 2). In contrast to manual measurement, an improved objective observation of the 3D vessel, as well as the possibility of the analysis of large volumes of data in a short time can be exploited. Based on the 3D surface model, highly resolved, time-dependent blood flow simulations using computational fluid dynamics were carried out in accordance with Berg *et al.*[28] We included the following boundary conditions: scaled flow rates at the inlet opening from a healthy volunteer,[29] pressure distribution at

the outlet openings,[30] and rigid vessel walls. Blood was treated as a Newtonian fluid (1055 kg/m³) with constant viscosity (4 mPa×s) and the flow was assumed to be laminar. For each case, the simulation of three cardiac cycles was performed, of which only the last cycle was included in the analysis of the 28 extracted hemodynamic parameters[21] (Figure 2, Table 2).

## Statistical analysis

For the determination of the best suited parameters based on their predictive power we conducted three phases of statistical evaluation using R version 3.5.3.

In the first phase of the statistical analysis, we analyzed the parameters in more detail with respect to differences between RIAs and UIAs. As each patient of our study harbored a RIA and at least one UIA, we tested the possible superiority of a multilevel model compared with hierarchical logistic regression analysis. If this was the case, a multilevel model was employed. Otherwise, deviation from normal distribution was tested based on histogram analysis in combination with skew and kurtosis values divided by two standard errors. Because significant values in large samples arise from even small deviations from normality, we decided on a threshold of 3.5. If the variables exceeded this threshold, they were transformed by means of logarithmization. Parameters with several equal (zero) values were analyzed with the nonparametric Wilcoxon rank-sum test, while the remaining parameters were evaluated with parametric Welch two sample *t*-test. The underlying dataset was screened with respect to outliers and plausibility of values. IAs were excluded from further analysis due to outliers (mean $\pm 4 \times$ standard deviation) in the data, which affected nine parameters of six aneurysms. Another IA was excluded due to a failure of the neck reconstruction.

For the second phase, correlation analysis between significant parameters from phase one was evaluated to identify independent parameters which do not correlate with each other. We used parametrical Pearson product-moment correlation for normally distributed parameters and nonparametrical Spearman's rank-sum correlation for non-normally distributed parameters.

In phase three, a hierarchical logistic regression analysis was performed based on the groups of parameters with low correlations. Parameters were added to the model in order of their importance, for example, effect size, calculated in phase one and included in the model if they improved its prediction quality. For the logistic regression analyses, we had to exclude four IAs, as not all parameter values (problems of parameter extraction occurred due to certain complex, highly irregular aneurysm morphologies) were present in all variables.

In order to provide a qualitative comparison with the current most well-established prediction model, we applied the PHASES score to our MIA patient collective. We calculated the PHASES

**Table 1.** Patients characteristics for all cases.

| Patient characteristics | *n* | Percentage |
|---|---|---|
| Male | 9 | 24% |
| Female | 29 | 76% |
| Hypertension | 24 | 63% |
| No hypertension | 14 | 37% |
| Age <70 years | 33 | 89% |
| Age ⩾70 years | 5 | 11% |
| **Localization of IA** | | |
| Anterior cerebral artery | 3 | 3% |
| Anterior communicating artery | 15 | 17% |
| Internal carotid artery | 13 | 15% |
| Middle cerebral artery | 30 | 35% |
| Posterior communicating artery | 11 | 13% |
| Basilar artery | 9 | 10% |
| Posterior cerebral artery | 2 | 2% |
| Others | 4 | 5% |
| **Number of IAs** | | |
| 2 IAs | 29 | 76% |
| 3 IAs | 7 | 18% |
| 4 IAs | 2 | 5% |
| | 87 | |

IA, intracranial aneurysm.

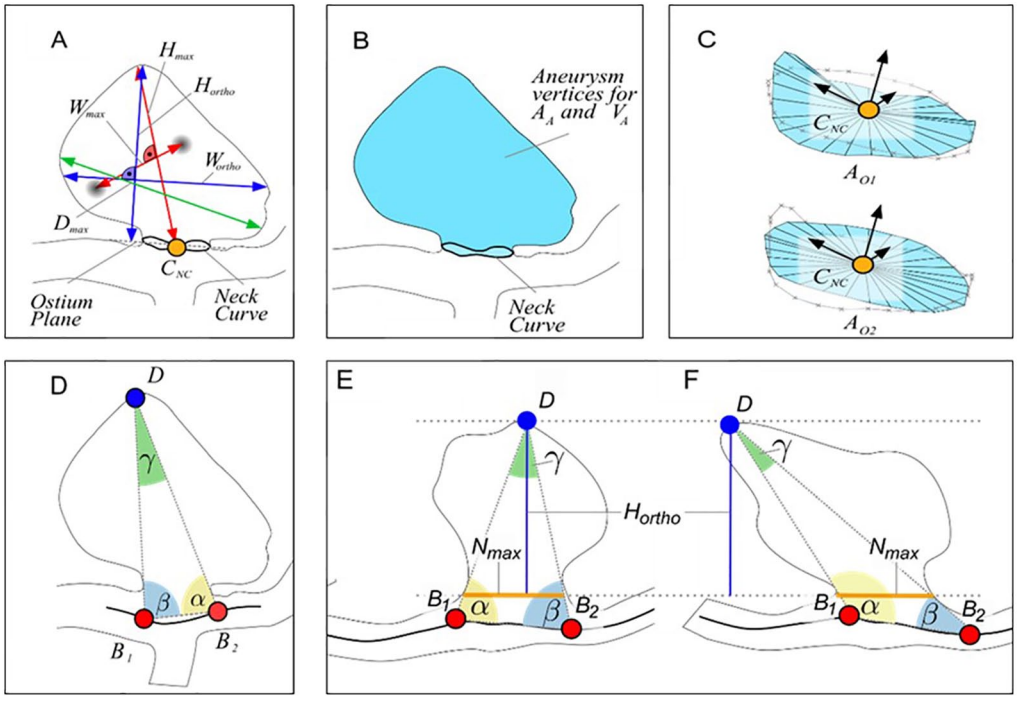


**Figure 1.** Illustration of the morphological parameters Hmax, Wmax, Hortho, Wortho and Dmax (a). The semi-automatically determined neck curve separates the aneurysm from the parent vessel surface mesh and area $A_A$ and volume $V_A$ of the aneurysm sac are extracted (b). The surface area of the ostium is extracted for the reconstructed neck curve (OA1) as well as for the projected neck curve (OA2) (c). The angle-related parameters account for the tilting of the aneurysm (d–f). Even if the aspect ratio is identical, γ and Δαβ differ (e, f).[27]
$A_A$, Surface area of the aneurysm.
$D_{max}$, Maximum diameter of the aneurysm.
$H_{max}$, Maximum height of the aneurysm.
$H_{ortho}$, Height of the aneurysm, measured vertically to the aneurysm neck.
$V_A$, Volume of the aneurysm.
$W_{max}$, Maximum width perpendicular to $H_{max}$.
$W_{ortho}$, Maximum width perpendicular to $H_{ortho}$.

score, as described by Greving *et al.*,[24] for the largest IA.

## Results

Significant differences between RIAs and UIAs were found in 13 out of 21 morphological parameters. However, the results show medium effects ($0.30 \leqslant r \leqslant 0.50$). Analysis of hemodynamic parameters yields differences between RIA and UIA for 3 out of 28 parameters. However, only one variable showed a medium effect (Aneurysm_RRT_max); other variables showed small effects.

In the second phase, we investigated the correlation of the 16 parameters identified in phase one using Spearman's rank-sum test. Morphological parameters showed a correlation with each other, with the exception of gamma ($0.05 < r < 0.30$) and AR1. Correlations between hemodynamic parameters showed medium and large effects. In terms of the correlation between morphological and hemodynamic parameters, Aneurysm_RRT_max and Aneurysm_RRT_mean showed the lowest correlations.

The presentation of the test statistics from the first and the second phase of the statistical analysis are published as online supplemental material.

Based on the results of phase two, we developed three models each containing two morphological and two hemodynamic parameters (which also exhibit a relatively low correlation to each other):

**Table 2.** List of the 21 morphological and 28 hemodynamic extracted parameters.[19–21,23,27]

| | Parameter | Definition |
|---|---|---|
| Morphological parameters | $H_{max}$ | Maximum height of the aneurysm |
| | $W_{max}$ | Maximum width perpendicular to $H_{max}$ |
| | $D_{max}$ | Maximum diameter of the aneurysm |
| | $H_{ortho}$ | Height of the aneurysm, measured vertically to the aneurysm neck |
| | $W_{ortho}$ | Maximum width perpendicular to $H_{ortho}$ |
| | $N_{max}$ | Maximum diameter of the aneurysm neck |
| | $N_{avg}$ | Average diameter of the aneurysm neck |
| | AR1 | Aspect ratio 1 ($H_{ortho}/N_{max}$) |
| | AR2 | Aspect ratio 2 ($H_{ortho}/N_{avg}$) |
| | EI | Ellipticity index (1–18^(1/3) $V_{CH}$^(2/3)/$A_{CH}$) |
| | NSI | Nonsphericity index (1–18^(1/3) V^(2/3)/$A_A$) |
| | UI | Undulation index (1–V/$V_{CH}$) |
| | $A_A$ | Aneurysm area (Surface area of the aneurysm) |
| | OA1 | Ostium area 1 (Area of the aneurysm ostium) |
| | OA2 | Ostium area 2 (Area of the aneurysm ostium with the neck curve projected onto a plane) |
| | $V_A$ | Volume of the aneurysm |
| | $V_{CH}$ | Volume of the convex hull of the aneurysm |
| | $A_{CH}$ | Surface area of the convex hull of the aneurysm |
| | Alpha | Angle at B1 describing angle from base line to the dome point |
| | Beta | Angle at B2 describing angle from base line to the dome point |
| | Gamma | Angle on the aneurysm dome depending on base points |
| Hemodynamic parameters | A_inflow | Area of the inflow at aneurysm ostium |
| | A_inflow_mean | Mean area of the inflow at aneurysm ostium |
| | NeckFlowRate | Flow rate that enters the aneurysm at a certain time point |
| | MeanNeckInflowRate | NeckFlowRate averaged over one cardiac cycle |
| | Q_vessel | Flow rate within the parent vessel |
| | Q_vessel mean | Mean flow rate within the parent vessel |
| | F_aneurysm | Shear stress of the aneurysm area |
| | F_high | Shear stress of the aneurysm area under high wall shear stress |
| | F_low | Shear stress of the aneurysm area under low wall shear stress |
| | Aneurysm_AWSS_mean | Mean average wall shear stress of the aneurysm |
| | Aneurysm_AWSS_max | Maximal average wall shear stress of the aneurysm |
| | A_high | Area of the aneurysm under high wall shear stress |
| | A_low | Area of the aneurysm under low wall shear stress |

*(Continued)*

**Table 2.** (Continued)

| | Parameter | Definition |
|---|---|---|
| | MeanAWSS_vessel | Mean average wall shear stress of the parent vessel |
| | VarianceAWSS_vessel | Variance of the wall shear stress of the parent vessel |
| | sdAWSS_vessel | Standard deviation of average wall shear stress occurring on the parent vessel |
| | AWSS_vessel_high | Abnormally high average wall shear stress on the parent vessel |
| | AWSS_vessel_low | Abnormally low average wall shear stress on the parent vessel |
| | Aneurysm_OSI_mean | Mean oscillatory shear index of the aneurysm |
| | Aneurysm_OSI_max | Maximal oscillatory shear index of the aneurysm |
| | Aneurysm_RRT_mean | Mean relative residence time of the aneurysm |
| | Aneurysm_RRT_max | Maximal relative residence time of the aneurysm |
| | ICI | Inflow concentration index |
| | ICI_mean | Mean inflow concentration index |
| | SCI | Shear concentration index |
| | HSI | High shear index |
| | LSI | Low shear index |
| | LSA | Low shear stress area percentage |

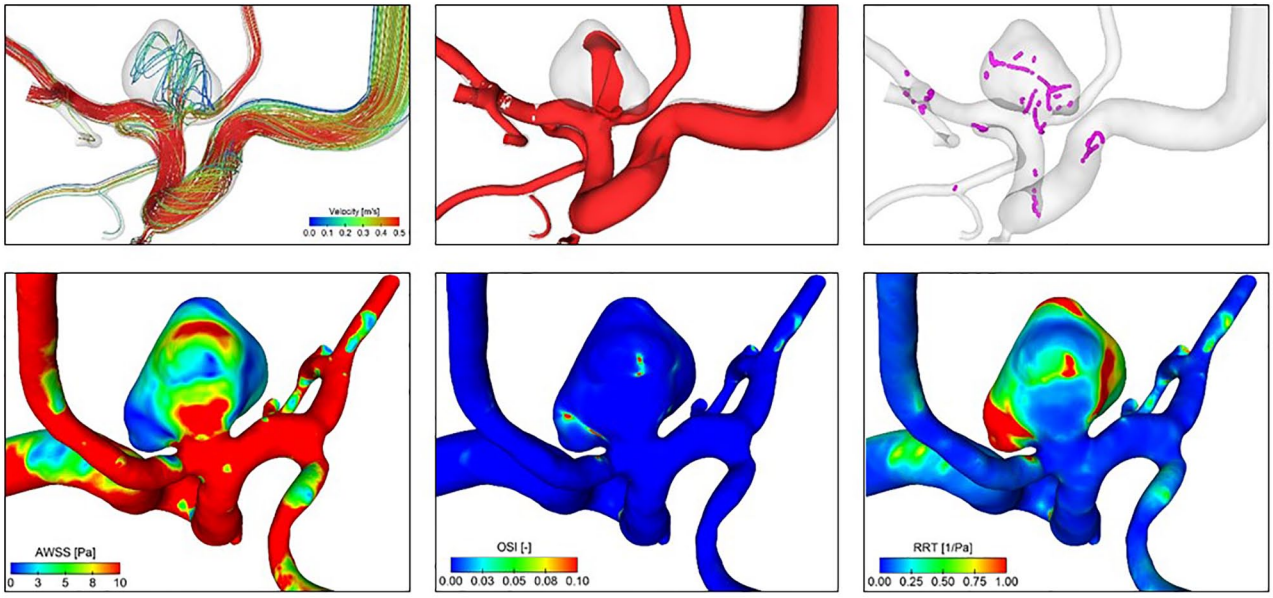


**Figure 2.** Exemplary illustration of relevant hemodynamic parameters. Upper row (flow visualization) from left to right: cycle-averaged streamlines color-coding the velocity magnitude; mean isosurface velocity highlighting occurring flow structures; vortex core lines revealing complex flow and the presence of interacting vortices. Lower row (hemodynamic surface forces) from left to right: cycle-averaged wall shear stress (AWSS); oscillatory shear index (OSI); relative residence time (RRT).

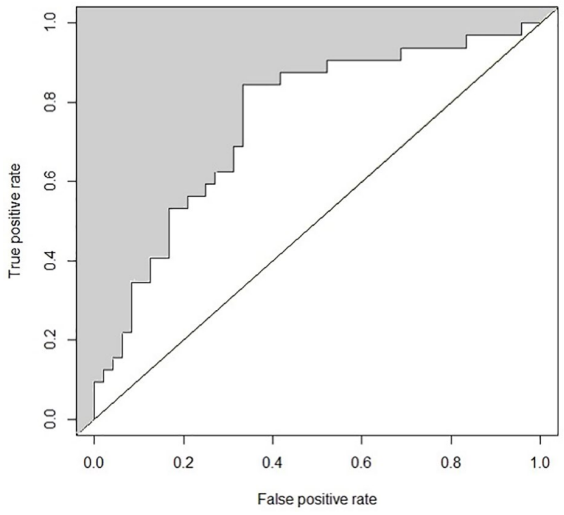


**Figure 3.** Presentation of the AUC (0.75) of the final model. AR1 and Aneurysm_RRT_max were the only parameters leading to the models' prediction quality regarding aneurysm rupture status. They account for 13% of the variance in the aneurysm rupture status.
Aneurysm_RRT_max, aneurysm maximal relative residence time; AR1, aspect ratio 1; AUC, area under the curve.

Model A: AR1, Aneurysm_RRT_max, $W_{ortho}$, A_low
Model B: AR1, $W_{ortho}$, Aneurysm_RRT_mean, A_low
Model C: $W_{ortho}$, gamma, Aneurysm_RRT_mean, A_low

In the third phase, we constructed the regression models using forward selection. We tested each model (Model A–C) for improvement of prediction quality by adding parameters. The analysis revealed a combination of two parameters (AR1, $p = 0.01$ and Aneurysm_RRT_max, $p = 0.04$) with significant improvement of the model. The AR1 was here defined as the height of the aneurysm neck measured vertically to the aneurysm neck ($H_{ortho}$) divided by the maximum diameter of the aneurysm neck ($N_{max}$), while the AR2 was defined as $H_{ortho}$ divided by the average diameter of the aneurysm neck ($N_{avg}$). Aneurysm_RRT_max describes the maximal relative residence time of the aneurysm. Both parameters account together for 13 % of the variance in the rupture status ($R^2 = 0.13$). The AUC of the final model was 0.75. (Figure 3).

Analysis of PHASES score distribution showed that 84% of the patients had a PHASES score of 0–6 points with an estimated 5-year rupture risk of <2%. We observed the following distribution of corresponding 5-year rupture risk in our patient cohort of patients with MIA: 47% of all patients had a 5-year rupture risk of <1%, 37% of all patients had a 5-year rupture risk of 1–1.9%, 11% of all patients had a 5-year rupture risk of 2–4.9% and 5% of all patients had a 5-year rupture risk of >5%. (Figure 4).

## Discussion

The concept of IAs as a homogenous disease is challenged by recent studies.[5,31–35] Among IA subgroups, MIAs constitute one of the most

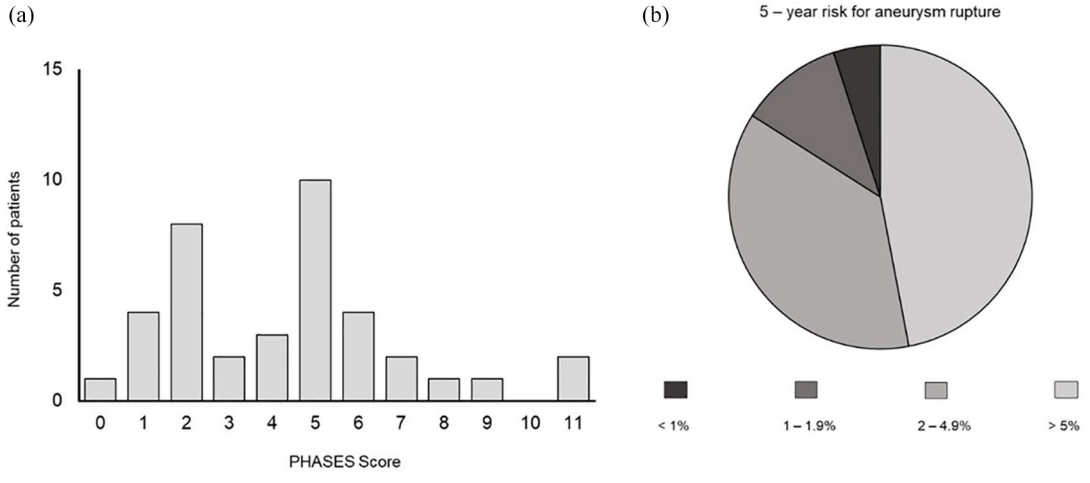


**Figure 4.** (a) Distribution of PHASES score, values. (b) Corresponding estimated 5-year risk for aneurysm rupture in patients with MIA.
MIA, multiple intracranial aneurysm.

important subgroups of patients harboring IAs, accounting for 20% of all IA patients.[5] In clinical practice, the presence of MIAs has an impact on treatment decisions.[36,37] Although, several studies elucidated the morphological and hemodynamic characteristics of MIA,[38–40] thus far a prediction model for MIAs has not been presented.

The PHASES score is established in the daily clinical practice in neurovascular centers; however, several limitations considering the rupture risk in the subgroup of MIAs are apparent. Although other studies already questioned the aneurysm size as the key parameter in rupture risk prediction,[41,42] the PHASES score still attributes this parameter as having the highest impact on aneurysm rupture. Furthermore, the PHASES score only integrates the cumulative rupture risk of patients with MIAs by taking earlier SAH into account. It is questionable whether this approach is able to reproduce the real cumulative rupture risk of patients with MIAs. Therefore, the introduction of a new prediction model based on morphological and hemodynamic parameters might lead to a better prediction.

As MIAs have the peculiarity of a location within the same patient, we aimed to use a nested comparison of IAs within the same patient. This approach would have been able to abbreviate the influence of patient characteristics on rupture risk of MIAs and lead to a stronger emphasis on morphological and hemodynamic characteristics. However, the application of a multilevel model only led in 6 of 49 parameters to a better model fit. Therefore, this finding implicates no significant impact of patients' characteristics on the prediction of aneurysm rupture in our cohort.

The first phase of our statistical analysis targeted the identification of morphological and hemodynamic parameters with high effect sizes in prediction of aneurysm rupture of MIA. With respect to that, we analyzed 49 (21 morphological and 28 hemodynamic) out of 81 established parameters[43] according to their significance level and, more importantly, to their effect sizes, revealing the precise parameter impact on the rupture risk. Although 13 morphological parameters and 3 hemodynamic parameters yielded significant results, they only achieved medium effect size. These findings suggest that a large number of introduced morphological and hemodynamic parameters show no significant results in the rupture risk assessment of MIAs. In addition, significant parameters seem to have only a medium effect on the rupture prediction in our patient collective. Despite the high number of parameters examined in this study, it is important to point out that we did not include all established parameters in our analysis. Especially those parameters considering the parent vessel were not automatically extracted by our semiautomatic neck curve reconstruction. Therefore, we are not able to draw any conclusions regarding the influence of these parameters on the rupture risk of MIAs in the context of this study. However, it should be mentioned that among the group of parameters including information about the parent vessel, the size ratio (aneurysm size divided by the average parent vessel diameter) shows significant associations with the rupture of IAs in numerous studies.[20,44–46]

As previously reported studies affirmed correlations between a small number of morphological and hemodynamic parameters,[17,20,47] we considered it a possible cause for the medium effect sizes achieved in phase one. A potential explanation for strong correlations between morphological and hemodynamic parameters might be that they are all size-related to some extent. In phase two of our statistical analysis in order to investigate this hypothesis, we performed an extended investigation of correlations between the calculated parameters. The analysis revealed strong correlations between morphological and hemodynamic parameters in general. In order to minimize the number of parameters included in the final prediction model, we aimed to select parameters with the comparatively lowest correlations coefficients. The six selected parameters still showed medium to high correlation coefficients in the majority of cases. Based on these results, we assume that the introduction of new parameters will only advance the rupture risk prediction if they exhibit low correlations with existing aneurysm size-related parameters.

The final hierarchical logistic regression revealed a prediction model for patients with MIAs based on two parameters (AR1 and Aneurysm_RRT_max). Although the results published here are based on an extensive and meticulously performed analysis, our final prediction model only achieved an AUC of 0.75. In connection with the results revealed by phase one and two of our statistical analysis, the only moderately high AUC,

along with the low number of parameters with independent impact on rupture risk prediction, raises the question of whether morphological analysis and blood flow simulations are capable of improving the rupture risk assessment of patients with MIAs. However, further studies including a higher number of patients need to be carried out to evaluate the real impact of morphology and hemodynamics on the rupture of MIAs.

## Limitations

There are several limitations related to the study design and the used methodology. The number of patients with MIAs investigated in this study is low, compared with other studies addressing rupture risk assessment of IAs in general. To obtain results with significance for the clinical routine, a higher number of cases needs to be included in further investigations. In addition, the underlying classification of an IA as unruptured or ruptured is not based on a prospective study. Therefore, there might be a bias due to the unknown natural progression of an unruptured IA, which means that it is unclear whether these aneurysms would have ruptured during follow up. Apart from this, uncertainty remains as to whether aneurysm rupture leads to changes in aneurysm morphology and, therefore, influences the morphological analysis. Our semiautomatic neck curve segmentation shows limitations in the analysis of aneurysms with particularly complex morphology. The exclusion of these aneurysms due to reconstruction failures had implications for the further statistical analysis presented in this study. Finally, the implemented boundary conditions were not patient specific due to a lack of availability of patient-specific information on exact flow conditions and *in vivo* local wall thickness differences.

## Conclusion

A high number of established morphological and hemodynamic parameters seem to have no or low effect on the prediction of aneurysm rupture in patients with MIAs. Moreover, meaningful parameters show a high amount of correlations between each other and seem to contain redundant information due to their relation to the aneurysm size. New parameters could improve the prediction accuracy if they are not aneurysm size-related. Consequently, for best possible rupture risk assessment of patients with MIAs, only the morphological parameter AR1 and the hemodynamic parameter Aneurysm_RRT_max need to be included in the prediction model.

## Acknowledgements

The authors thank Dr. Maria Luz for conducting the statistical analysis.

## Author's contributions

- Data acquisition: BN, VMS, SS
- Data analysis: BN, VMS, SS, PB, MS, JH, OB, KPS
- Conception and design of study: BN, SS, PB, MS, IES, BP
- Writing of manuscript: BN, VMS, SS

## Funding

The authors disclosed receipt of the following financial support for the research, authorship, and/or publication of this article: This study was partly funded by the Federal Ministry of Education and Research (grant number 13GW0095A) and the German Research Foundation (grant number SA 3461/2-1, BE 6230/2-1).

## Conflict of interest statement

The authors declare that there is no conflict of interest.

## Ethics statement

The ethics committee waivered the need for ethics approval due to the retrospective implementation of the study.

## ORCID iD

Belal Neyazi https://orcid.org/0000-0002-3163-0545

## Supplemental material

Supplemental material for this article is available online.

## References

1. Vlak MH, Algra A, Brandenburg R, *et al.* Prevalence of unruptured intracranial aneurysms, with emphasis on sex, age, comorbidity, country, and time period: a systematic review and meta-analysis. *Lancet Neurol* 2011; 10: 626–636.
2. Molyneux A, Kerr R, Stratton I, *et al.* International Subarachnoid Aneurysm Trial (ISAT) of neurosurgical clipping versus

endovascular coiling in 2143 patients with ruptured intracranial aneurysms: a randomised trial. *Lancet Lond Engl* 2002; 360: 1267–1274.

3. Wiebers DO, Whisnant JP, Huston J, *et al.* Unruptured intracranial aneurysms: natural history, clinical outcome, and risks of surgical and endovascular treatment. *Lancet Lond Engl* 2003; 362: 103–110.
4. Nieuwkamp DJ, Setz LE, Algra A, *et al.* Changes in case fatality of aneurysmal subarachnoid haemorrhage over time, according to age, sex, and region: a meta-analysis. *Lancet Neurol* 2009; 8: 635–642.
5. Jabbarli R, Dinger TF, Darkwah Oppong M, *et al.* Risk factors for and clinical consequences of multiple intracranial aneurysms: a systematic review and meta-analysis. *Stroke* 2018; 49: 848–855.
6. Ostergaard JR and Høg E. Incidence of multiple intracranial aneurysms. Influence of arterial hypertension and gender. *J Neurosurg* 1985; 63: 49–55.
7. Qureshi AI, Suarez JI, Parekh PD, *et al.* Risk factors for multiple intracranial aneurysms. *Neurosurgery* 1998; 43: 22–26; discussion 26–27.
8. Juvela S. Risk factors for multiple intracranial aneurysms. *Stroke* 2000; 31: 392–397.
9. Brown RD and Broderick JP. Unruptured intracranial aneurysms: epidemiology, natural history, management options, and familial screening. *Lancet Neurol* 2014; 13: 393–404.
10. Rinkel GJ, Djibuti M, Algra A, *et al.* Prevalence and risk of rupture of intracranial aneurysms: a systematic review. *Stroke* 1998; 29: 251–256.
11. Guan J, Karsy M, Couldwell WT, *et al.* Factors influencing management of unruptured intracranial aneurysms: an analysis of 424 consecutive patients. *J Neurosurg* 2017; 127: 96–101.
12. Burns JD, Huston J, Layton KF, *et al.* Intracranial aneurysm enlargement on serial magnetic resonance angiography: frequency and risk factors. *Stroke* 2009; 40: 406–411.
13. Juvela S, Poussa K, Lehto H, *et al.* Natural history of unruptured intracranial aneurysms: a long-term follow-up study. *Stroke* 2013; 44: 2414–2421.
14. Matsumoto K, Oshino S, Sasaki M, *et al.* Incidence of growth and rupture of unruptured intracranial aneurysms followed by serial MRA. *Acta Neurochir (Wien)* 2013; 155: 211–216.
15. Yasui N, Suzuki A, Nishimura H, *et al.* Long-term follow-up study of unruptured intracranial aneurysms. *Neurosurgery* 1997; 40: 1155–1159; discussion 1159–1160.
16. Raghavan ML, Ma B and Harbaugh RE. Quantified aneurysm shape and rupture risk. *J Neurosurg* 2005; 102: 355–362.
17. Dhar S, Tremmel M, Mocco J, *et al.* Morphology parameters for intracranial aneurysm rupture risk assessment. *Neurosurgery* 2008; 63: 185–196; discussion 196–197.
18. Kleinloog R, de Mul N, Verweij BH, *et al.* Risk factors for intracranial aneurysm rupture: a systematic review. *Neurosurgery* 2018; 82: 431–440.
19. Lee S-W, Antiga L and Steinman DA. Correlations among indicators of disturbed flow at the normal carotid bifurcation. *J Biomech Eng* 2009; 131: 061013.
20. Xiang J, Natarajan SK, Tremmel M, *et al.* Hemodynamic-morphologic discriminants for intracranial aneurysm rupture. *Stroke* 2011; 42: 144–152.
21. Cebral JR, Mut F, Weir J, *et al.* Quantitative characterization of the hemodynamic environment in ruptured and unruptured brain aneurysms. *AJNR Am J Neuroradiol* 2011; 32: 145–151.
22. Lu G, Huang L, Zhang XL, *et al.* Influence of hemodynamic factors on rupture of intracranial aneurysms: patient-specific 3D mirror aneurysms model computational fluid dynamics simulation. *AJNR Am J Neuroradiol* 2011; 32: 1255–1261.
23. Xiang J, Tutino VM, Snyder KV, *et al.* CFD: computational fluid dynamics or confounding factor dissemination? The role of hemodynamics in intracranial aneurysm rupture risk assessment. *AJNR Am J Neuroradiol* 2014; 35: 1849–1857.
24. Greving JP, Wermer MJH, Brown RD, *et al.* Development of the PHASES score for prediction of risk of rupture of intracranial aneurysms: a pooled analysis of six prospective cohort studies. *Lancet Neurol* 2014; 13: 59–66.
25. Detmer FJ, Chung BJ, Mut F, *et al.* Development and internal validation of an aneurysm rupture probability model based on patient characteristics and aneurysm location, morphology, and hemodynamics. *Int J Comput Assist Radiol Surg* 2018; 13: 1767–1779.
26. Saalfeld S, Berg P, Neugebauer M, *et al.* Reconstruction of 3D surface meshes for blood flow simulations of intracranial aneurysms. In: *Konference*

*für Computer- und Roboterassistierte Chirurgie (CURAC)*, Bremen, Germany, 2015.

27. Saalfeld S, Berg P, Niemann A, *et al.* Semiautomatic neck curve reconstruction for intracranial aneurysm rupture risk assessment based on morphological parameters. *Int J Comput Assist Radiol Surg* 2018; 13: 1781–1793.
28. Berg P, Saalfeld S, Voß S, *et al.* A review on the reliability of hemodynamic modeling in intracranial aneurysms: why computational fluid dynamics alone cannot solve the equation. *Neurosurg Focus* 2019; 47: E15.
29. Berg P, Stucht D, Janiga G, *et al.* Cerebral blood flow in a healthy Circle of Willis and two intracranial aneurysms: computational fluid dynamics versus four-dimensional phase-contrast magnetic resonance imaging. *J Biomech Eng* 2014; 136: 041003.
30. Chnafa C, Brina O, Pereira VM, *et al.* Better than nothing: a rational approach for minimizing the impact of outflow strategy on cerebrovascular simulations. *AJNR Am J Neuroradiol* 2018; 39: 337–343.
31. Strother CM and Jiang J. Intracranial aneurysms, cancer, x-rays, and computational fluid dynamics. *AJNR Am J Neuroradiol* 2012; 33: 991–992.
32. Lv N, Tang H, Chen S, *et al.* Morphological parameters related to aneurysm wall enhancement in patients with multiple intracranial aneurysms. *World Neurosurg* 2018; 114: e338–e343.
33. Christiano LD, Gupta G, Prestigiacomo CJ, *et al.* Giant serpentine aneurysms. *Neurosurg Focus* 2009; 26: E5.
34. Zhou Z, Xu Y, Delcourt C, *et al.* Is regular screening for intracranial aneurysm necessary in patients with autosomal dominant polycystic kidney disease? A systematic review and meta-analysis. *Cerebrovasc Dis Basel Switz* 2017; 44: 75–82.
35. Dengler J, Heuschmann PU, Endres M, *et al.* The rationale and design of the Giant Intracranial Aneurysm Registry: a retrospective and prospective study. *Int J Stroke Off J Int Stroke Soc* 2011; 6: 266–270.
36. Etminan N, Brown RD, Beseoglu K, *et al.* The unruptured intracranial aneurysm treatment score: a multidisciplinary consensus. *Neurology* 2015; 85: 881–889.
37. Dong Q-L, Gao B-L, Cheng Z-R, *et al.* Comparison of surgical and endovascular approaches in the management of multiple intracranial aneurysms. *Int J Surg Lond Engl* 2016; 32: 129–135.
38. Zhang Y, Yang X, Wang Y, *et al.* Influence of morphology and hemodynamic factors on rupture of multiple intracranial aneurysms: matched-pairs of ruptured-unruptured aneurysms located unilaterally on the anterior circulation. *BMC Neurol* 2014; 14: 253.
39. Jing L, Fan J, Wang Y, *et al.* Morphologic and hemodynamic analysis in the patients with multiple intracranial aneurysms: ruptured versus unruptured. *PLoS One* 2015; 10: e0132494.
40. Berg P and Beuing O. Multiple intracranial aneurysms: a direct hemodynamic comparison between ruptured and unruptured vessel malformations. *Int J Comput Assist Radiol Surg* 2018; 13: 83–93.
41. Clarke M. Systematic review of reviews of risk factors for intracranial aneurysms. *Neuroradiology* 2008; 50: 653–664.
42. Sonobe M, Yamazaki T, Yonekura M, *et al.* Small unruptured intracranial aneurysm verification study: SUAVe study, Japan. *Stroke* 2010; 41: 1969–1977.
43. Liang L, Steinman DA, Brina O, *et al.* Towards the clinical utility of CFD for assessment of intracranial aneurysm rupture - a systematic review and novel parameter-ranking tool. *J Neurointerventional Surg* 2019; 11: 153–158.
44. Mocco J, Brown RD, Torner JC, *et al.* Aneurysm morphology and prediction of rupture: an international study of unruptured intracranial aneurysms analysis. *Neurosurgery* 2018; 82: 491–496.
45. Kashiwazaki D and Kuroda S Sapporo SAH Study Group. Size ratio can highly predict rupture risk in intracranial small (<5mm) aneurysms. *Stroke* 2013; 44: 2169–2173.
46. Rahman M, Smietana J, Hauck E, *et al.* Size ratio correlates with intracranial aneurysm rupture status: a prospective study. *Stroke* 2010; 41: 916–920.
47. Ryu C-W, Kwon O-K, Koh JS, *et al.* Analysis of aneurysm rupture in relation to the geometric indices: aspect ratio, volume, and volume-to-neck ratio. *Neuroradiology* 2011; 53: 883–889.